Two Very Efficient Nonlinear Laser Absorption Mechanisms in Clusters

P. Mulser,[1,*] M. Kanapathipillai,[2,†] and D. H. H. Hoffmann[2]

[1]*Theoretical Quantum Electronics (TQE), Darmstadt University of Technology, Schlossgartenstrasse 7, 64289 Darmstadt, Germany*
[2]*Gesellschaft für Schwerionenforschung, Planckstrasse 1, D-64291, Darmstadt, Germany*

(Received 13 October 2004; published 2 September 2005)

Experiments show strongly enhanced absorption of ultrashort superintense laser beams in clustered matter in the so-called collisionless regime. Despite numerous particle in cell simulations confirming this behavior, the underlying physical processes are not sufficiently clear. The familiar linear resonance absorption does not apply as long as the plasma frequency exceeds that of the laser. However, we show here that with increasing laser intensity the oscillations become nonlinear and can enter into resonance with the laser frequency because of restoring force lowering in Coulomb systems. Excellent absorption already at moderate intensities is the consequence. The other absorption mechanism we analyze explicitly consists in the coherent superposition of electron-ion collisions in ionized clusters. Collisional absorption enhancement factors of several orders of magnitude are found.

DOI: 10.1103/PhysRevLett.95.103401 PACS numbers: 36.40.Gk, 52.25.Os, 52.50.Jm

Efficient intense laser-matter coupling in clustered media is a well-established experimental fact [1]. The physical understanding of the interaction is satisfactory in the multiphoton and field ionization phase [2,3]. With the generation of a sufficient electron concentration, collisions become important for heating. However, as the kinetic electron temperature T_e approaches 500–1000 eV collisional absorption becomes inefficient. Nevertheless, in the subsequent so-called collisionless regime, light absorption still continues, generally to an extent as to produce most of the heating during this phase, as solidly confirmed by particle in cell (PIC) and molecular dynamic simulations [2–7]. They show an increase in absorption by orders of magnitude when the molecules of a gas combine to clusters. It is this stage for which analytical modeling is poor and physical understanding is unsatisfactory. Basically in the collisionless regime there exists the model of linear resonance absorption. which consists in the resonant excitation of plasmons at the rarefying edge of larger clusters and small droplets [8], or in linear Mie resonances occurring at $\omega_p/\sqrt{3}$, ω_p plasma frequency [9]. With the ultrashort laser pulses, typically shorter than 100 fs, this model does not work with the fundamental laser frequency ω owing to $\omega \ll \omega_p$, perhaps, however, with one of its weak higher harmonics (3ω in [10]).

Here we present two ''collisionless'' absorption mechanisms, both of which derive their high efficiency from nonlinearities. One of them is based on nonlinear resonance, i.e., lowering of the resonance frequency with increasing oscillation amplitude. The second takes advantage of the possibility of coherent superposition of electron-ion collisions in clusters. The principle of the first mechanism is very simple and, somehow, resembles aspects of nonlinear Landau damping. Consider the potential Φ of two interpenetrating spheres of positive (ions) and negative (electrons) charges (Fig. 1). At low energy of excitation the potential is harmonic with eigenfrequency $\omega_0 = \omega_p/\sqrt{3} \gg \omega$. As the amplitude increases Φ widens, i.e., the restoring force $-\nabla\Phi$ becomes weaker than that of the linear oscillator (parabola in Fig. 1, dashed line). As a consequence ω_0 decreases and, at a well-defined excitation energy, it becomes equal to ω and hence resonance absorption can start. In this Letter a compressed, computer aided proof of this statement is given.

We consider a cluster consisting of ion and electron spheres of radii R_i and $R_e \geq R_i$, uniformly distributed charges q_i and $-q_e = N_e e \leq q_i$, located at $\boldsymbol{x}_i$ and $\boldsymbol{x}_e$, respectively, [11,12]. Further, we introduce the following variables: $\boldsymbol{e}_r = \boldsymbol{x}/|\boldsymbol{x}|$, $\boldsymbol{x} = \boldsymbol{x}_e - \boldsymbol{x}_i$, $\boldsymbol{v} = \frac{d\boldsymbol{x}}{dt}$, $r = |\boldsymbol{x}|/R_e$, $\rho = R_i/R_e$. The electron sphere oscillates according to

$$\frac{m_e d\gamma \boldsymbol{v}}{dt} = \boldsymbol{f}(\boldsymbol{x}) - e(\boldsymbol{E} + \boldsymbol{v} \times \boldsymbol{B}); \quad \gamma = \left(1 - \frac{v^2}{c^2}\right)^{-1/2}, \quad (1)$$

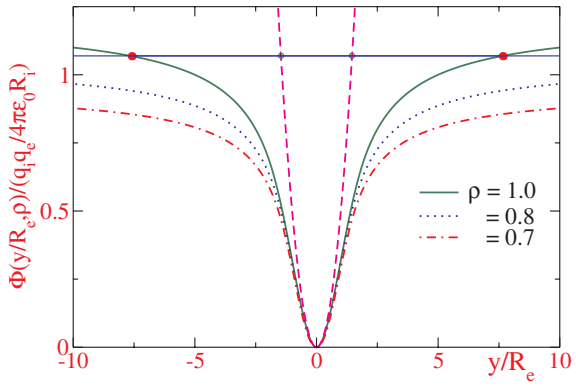

FIG. 1 (color online). Spherical potential $\Phi(y = r)$ of the nonlinear oscillator equation (1) for various values of $\rho = R_i/R_e$; q_e, q_i charges of electron and ion spheres of radii R_e, R_i. The parabola (dashed line) is the associated harmonic potential. At low oscillation amplitude the eigenfrequencies are equal, at large amplitudes the eigenfrequency of $\Phi(r)$ tends to zero. Observe the turning points indicated for the normalized excitation energy 1.07.

where $N_e \boldsymbol{f}(\boldsymbol{x}) = -\nabla\Phi$ is the Coulomb attraction of the interpenetrating spheres. It is proportional to r for either $r \leq 1-\rho$ or $r \ll 1$ (parabolic), Coulomb-like for the spheres separated from each other, $r > 1+\rho$, and a polynomial function of powers r^{-2}, r, r^2, r^4 in between (see Fig. 1). For large amplitudes ω_0 approaches zero. This means that with a laser pulse $\boldsymbol{E} = \boldsymbol{e}_y E_0 g(x,t)$, $g(x,t) = \sin[(\omega t - kx)/n]\sin[(\omega t - kx)]$, $n/2$ cycles long, peak intensity $I_0 = \epsilon_0 c E_0^2/2$ and magnetic field $\boldsymbol{B} = \boldsymbol{e}_z B$, $B = E/c$, at high intensity the threshold for resonance $I_0 = I_{\rm res}$ is reached, i.e., $\omega_0(I_{\rm res}) = \omega$. The absorbed energy e_a per electron as a function of laser peak intensity I_0 is shown in Fig. 2 for pulses $n/2 = 10$ cycles long, $\omega = 0.227\omega_0$ (Ti:Sapphire laser), and a large cluster of radius $R_e = R_i = R = 10$ nm and electron density $n_e = 10^{23}$ cm^{-3} (solid line). Before resonance ($I_0 < I_{\rm res}$) there is almost no energy absorption. A strong, ramplike and, finally, steplike increase of e_a by more than 5 orders of magnitude altogether occurs around $I_0 = I_{\rm res} \approx 6.78 \times 10^{17}$ W cm^{-2} where $\omega_0 = 2\pi/T = \omega$ at the pulse maximum. Beyond resonance ($I_0 > I_{\rm res}$) e_a, apart from some fine structure, remains constant. Almost the same result is obtained with 20 and 30 cycles long pulses. For comparison, the dotted straight line refers to the harmonic oscillator of eigenfrequency $\omega_0 = \omega_p/\sqrt{3}$. Since it never crosses the resonance (almost) no absorption is observed. Comparison of the solid and dot-dashed lines ($\boldsymbol{B} = 0$) shows that the Lorentz force has only a slight influence on resonance, i.e., on the amount of the absorbed energy. The evolution in time of the quiver velocity $\gamma v_y(t) \simeq v_y(t)$, $e_a(t) = -e\int^t v_y E dt'$, and the local value of the driving E_y field are plotted in Fig. 3 at the resonance threshold $I_0 = I_{\rm res} = 6.78 \times 10^{17}$ W cm^{-2} and $n/2 = 10$. The signature of the resonance is a phase shift $\Delta\varphi = \pi$ between $E_y(t)$ and $v_y(t)$. In Fig. 3 it occurs during one laser period T_L between $t/T_L = 6.6$ and 7.6, as seen (i) from the sudden increase of $e_a(t)$ just in this interval and (ii) by following the phase difference of $\gamma v_y(t)$ relative to $E_y(t)$ in the interval (0, 10 T_L). Starting form the left-hand side, one observes that the sinusoidal shape of γv_y is perturbed in its maxima and minima by the 2ω periodicity of the Lorentz force which results in local minima and maxima on the top of the fundamental maxima and minima. The exact position of the latter appear after inverting the sign of the Lorentz minima and maxima; in particular, the last fundamental maximum before resonance lies at $t/T_L = 6.6$, coincident with the local Lorentz minimum. Its phase shift relative to $E = E_y(t)$ is $\pi/2$. At $t/T_L = 7.6$ there is the next fundamental minimum of γv_y located $\pi/2$ ahead of $E_y(t)$, and the following maximum of γv_y is located ahead by $3\pi/2$. Owing to this shift at resonance the Lorentz contribution becomes small and (nearly) invisible for $t/T_L > 7.3$. A large fraction of $e_a(t)$ is reversible, the net absorption (irreversible part) is $e_a = e_a(t > nT_L/2)$ after the pulse has ended. Figure 3 also shows the important facts that asymmetric excitation and nonlinearities (on T_L time scale) out of resonance do not contribute to absorption.

Spatial nonuniformities of the Coulomb field cause tidal forces on the electron cloud: the electron sphere begins to expand and disintegrates; single electrons drift away. To

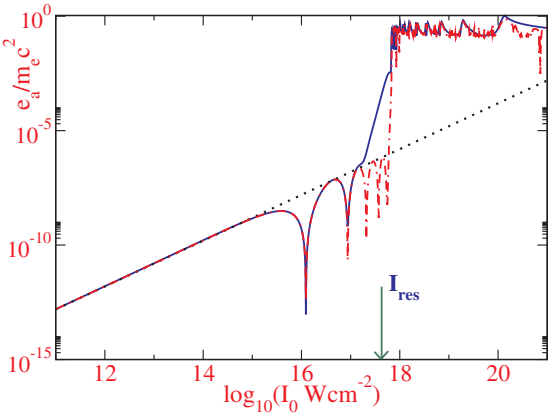

FIG. 2 (color online). Energy absorption of the nonlinear oscillator equation (1) from a sine laser pulse. $R_e = R_i = 10$ nm, $\omega/\omega_0 = 0.227$. The absorbed energy per electron e_a at the end of the pulse in units of its rest energy $m_e c^2$ is shown as a function of peak laser intensity I_0 in W cm^{-2} for pulses containing $n/2 = 10$ laser cycles with (solid line) and without Lorentz force (dot-dashed line). At the resonance point $I_0 = I_{\rm res} = 6.78 \times 10^{17}$ W cm^{-2} (B included), e_a increases by more than 2 orders of magnitude. If only the harmonic term is kept in (1) (parabola in Fig. 1) absorption remains extremely small (dotted line).

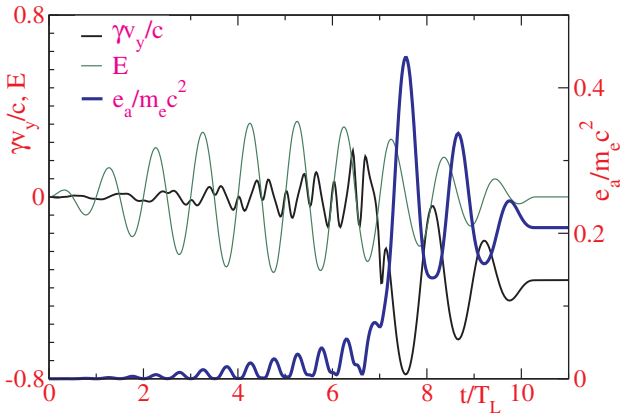

FIG. 3 (color online). Temporal evolution of the oscillator equation (1) at the resonance threshold $I_{\rm res} = 6.78 \times 10^{17}$ W cm^{-2}: laser field E (thin solid line), quiver velocity γv_y, and absorbed energy per electron $e_a(t)$ (bold line). Lorentz factor $\gamma = 1/(1 - v_x^2/c^2 - v_y^2/c^2)^{1/2}$, c light velocity, $m_e c^2$ rest energy; $\omega/\omega_0 = 0.227$, $T_L = 2\pi/\omega$. From $t \approx 6.6T_L$ to $t \approx 7.6T_L$ the phase of v_y changes by π with respect to the driver field E. The periodicity of 2ω superposed on the ω periodicity in v_y is due to the Lorentz force. At $t \gtrsim 7T_L$ a drift is superposed on v_y (outer ionization).

prove our assertion on resonant energy gain also for single electrons and expanding clusters, we investigated the following two variants of the rigid oscillator: (i) energy gain of test particles starting from various positions inside the cluster, (ii) resonant behavior of the rigid oscillator under the uniform expansion of the electron sphere according to $R_e(t) = R_i + vt$, with v varying between the ion and electron thermal velocity. In both cases our assertion is confirmed. Although the combined field of the laser and laser-induced space charge is complex, the test electron dynamics is nearly identical with that of the rigid oscillator of Fig. 3 with respect to resonance behavior: energy gain $e_a > 0$ when the resonance point $\omega_0(I_{\rm res}) = \omega$ is crossed, $e_a \approx 0$ at all values of $\omega < \omega_0$. The main difference is that now each test electron enters into resonance at a different value of $I_{\rm res}$.

We summarize the numerical investigations as follows: (1) Nonlinear resonance of entire bunches of electrons and of single particles is a leading mechanism of collisionless absorption. (2) Almost no irreversible energy gain (''heating'') takes place out of resonance. (3) Tidal forces soften and widen the non-resonant–resonant transition. (4) The $\boldsymbol{v} \times \boldsymbol{B}$ force merely leads to a more isotropic electron velocity distribution. (5) The resonant threshold $I_{\rm res}$ is proportional to the square of the cluster radius.

The second mechanism whose efficiency we analyze here explicitly is due to the coherent superposition of collisions in clusters. The underlying idea goes back to a proposal for an alternative heating mechanism one of us made at a Varenna Internationl Conference in 1997 in connection with two papers on absorption [13,14]. The absorption coefficient α, due to collisions in a plasma, is proportional to the ion density n_i and the square of the ion charge, $\alpha \sim Z_i^2 n_i$. When N ions cluster together the density of scatterers n_C decreases by N, but their charge increases by $Z_i N$ resulting in an increase of $\alpha \sim N$. A rough estimate of multiplication factors of α under simplified conditions (isotropic electron distribution, Born approximation, total outer ionization) were presented in [15].

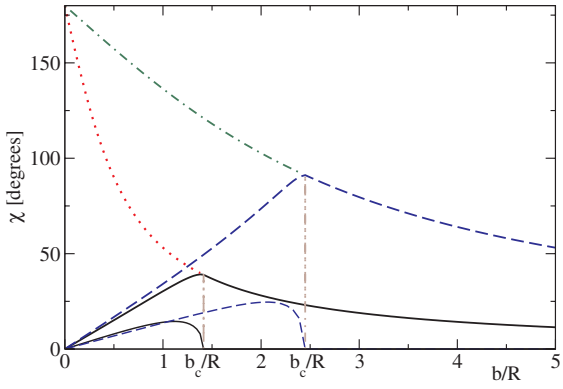

FIG. 4 (color online). Scattering angle χ as a function of the impact parameter b for a uniformly charged spherical cluster. Bold dashed curve for $b_\perp = 2.5R$, and solid curve for $b_\perp = 0.5R$, R cluster radius. The corresponding deflections inside the cluster are indicated by the thin dashed and solid lines ending at their respective $b = b_{\rm c}$ points. The dot-dashed and the dotted lines starting from $\chi = 180°$ refer to Coulomb scattering from a point charge q.

The calculation of the time dependent enhancement of inverse bremsstrahlung due to clustering is complex. The aim here is to show that in a laser-cluster interaction experiment of standard type, collective inverse bremsstrahlung is a leading absorption mechanism also in the so-called collisionless stage. In order to obtain realistic amplification factors of collisional absorption due to clustering $g = \alpha_C/\alpha$, α_C absorption coefficient of the cluster medium, the fraction ξ of ions combining to clusters, their ''outer ionization'' degree η_C; i.e., the net charge of the cluster, and the collision frequency ν_{eC} of an electron with the cluster gas in the presence of the intense laser field (see for instance [16]) need to be known. It holds

$$\nu_{eC} = \xi \eta_C^2 \frac{Z_C}{Z_i} \frac{L_C}{\ln\Lambda_{\rm ei}} \nu_{\rm ei}, \qquad \alpha_{eC} = \frac{\nu_{eC}}{c} \frac{\omega_p^2}{\omega^2}. \quad (2)$$

Λ_{ei} is the Coulomb logarithm of the plasma ions and L_C is the generalized Coulomb logarithm of the clusters. The Coulomb scattering angle χ is a function of the impact parameter b. For $b > b_c = R(1 + 2b_\perp/R)^{1/2}$, $\chi(b = b_\perp) = \pi/2$, it coincides with the Rutherford scattering angle; for orbits crossing the cluster, $b \le b_{\rm c}$, it behaves as shown in Fig. 4. L_C is calculated from $L_C = \frac{1}{2}\int_0^{b_c}(1 - \cos\chi) b db/R^2 + \frac{1}{2}\ln[(b_\perp^2 + b_{\rm max}^2)/(b_\perp^2 + b_c^2)]$, with $b_{\rm max} = (\hat{v}_{\rm os}^2/4 + v_{\rm th}^2)^{1/2}/\omega_p$, $\hat{v}_{\rm os} = eE/m_e\omega$, $v_{\rm th} = \sqrt{T_e/m_e}$, and the integral term to be evaluated numerically.

Assume that the fraction ξ of atoms of a hydrogen plasma of density 10^{20} cm^{-3} forms clusters of radius $R = 1$, $R = 5$, $R = 10$, and $R = 20$ nm; the rest remains as a uniform background gas. The clusters are assumed to be totally ionized (''inner ionization''). The additional parameters chosen are $T_e = 1$ and 20 keV and $I \le 10^{15}$, 10^{17}, and $I = 10^{18}$ W cm^{-2}; and $\lambda = 800$ nm (Ti:Sapphire laser). A lower limit of η_C is determined under the assumption that the electrons in which the single cluster is embedded are in thermal equilibrium [17]. The additional effect of $\hat{v}_{\rm os}$ on η_C is ignored (no quantitative analysis yet available). The collision frequency $\nu_{\rm ei}$ is pre-

TABLE I. Electron-ion collision frequency in fully ionized hydrogen plasma at two temperatures $T_e = 1$ and 20 keV and ion density $n_i = 10^{20}$ cm^{-3} for various laser intensities.

I[W cm^{-2}]	$T_e = 1$ keV		$T_e = 20$ keV	
	$\ln\Lambda_{\rm ei}$	$\nu_{\rm ei}$[s^{-1}]	$\ln\Lambda_{\rm ei}$	$\nu_{\rm ei}$[s^{-1}]
$\le 10^{15}$	6.7	1.7×10^{11}	9.4	1.7×10^{9}
$\le 10^{17}$	8.2	1.3×10^{10}	9.6	1.2×10^{9}
$\le 10^{18}$	10.3	1.2×10^{9}	10.7	3.9×10^{8}

TABLE II. Generalized Coulomb logarithm L_C and amplification factors $g = \nu_{eC}/\nu_{ei}$ for relevant parameters.

			$T_e = 1$ keV			$T_e = 20$ keV		
R nm	Z_C	I W cm^{-2}	η_C	L_C	g	η_C	L_C	g
1	210	$\leq 10^{15}$		2.1	66		3.5	79
		10^{17}	1.0	3.0	77	1.0	3.7	80
		10^{18}		3.0	61		5.2	103
5	2.6×10^4	$\leq 10^{15}$		0.1	4.1×10^2		1.6	4.4×10^3
		10^{17}	0.98	0.8	2.3×10^3	1.0	1.7	4.7×10^3
		10^{18}		1.3	3.2×10^3		3.5	8.6×10^3
10	2.1×10^5	$\leq 10^{15}$		0.1	4.9×10^2		0.6	1.4×10^4
		10^{17}	0.43	0.2	9.5×10^2	1.0	0.7	1.6×10^4
		10^{18}		0.3	1.3×10^3		2.8	3.4×10^4
20	1.7×10^6	$\leq 10^{15}$		0.05	3.8×10^2		0.12	2.2×10^4
		10^{17}	0.17	0.15	8.9×10^2	1.0	0.12	2.1×10^4
		10^{18}		0.33	1.6×10^3		1.5	2.3×10^4

sented in Table I for relevant parameters with the correct quantum cutoffs according to the most advanced quantum kinetic formulas [18], critically evaluated by summing up to 500 terms to ensure convergence at large $\hat{v}_{os}/v_{th}$ ratios; at $\hat{v}_{os}/v_{th} > 4.8$, b_{max} saturates [19]. For $b_{max} < b_c$, one has to set $b_{max} = b_c$. The resulting amplification factors are given in Table II. Values for g as high as 2.3×10^5 are obtained. The main deviation from $g \sim Z_C$ (or N) originates from the quadratic dependence of g on η_C and from L_C ranging from $L_C = 0.05$ to $L_C = 5.2$. With $n_i = 10^{18}$ cm^{-3}, ν_{ei} decreases approximately by a factor of 80 and g increases by 10%–20%. To illustrate the impact of clustering on absorption we determine the absorption length $L_a = 1/\alpha$, $\alpha = \nu_{ei}\omega_p^2/(c\omega^2)$ for $R = 10$ nm, $I = 10^{17}$ W cm^{-2}, $T_e = 20$ keV from Table II. For the hydrogen gas it is $L_a = 4.4$ m. After perfect clustering ($\xi = 1$) it shrinks to $L_{a,c} = L_a/g = 272$ μm. For $I = 10^{18}$ W cm^{-2} from the last line in Table II $L_a = 13.4$ m shrinks to $L_a/g = 58$ μm.

In conclusion it has been shown (i) that due to the quadratic dependence of the electron-ion collision frequency ν_{ei} on the charge number Z of the scatterer, there may occur a giant enhancement of this quantity by many orders of magnitude if Z can be increased correspondingly, as, for example, in clusters, aerosols, sprays, and small droplets of liquids, all of them with $R \ll \lambda$. (ii) The effect is relevant to light absorption in dusty plasmas. At low laser intensities or high frequencies (x-ray lasers) the g factors for $I \leq 10^{15}$ W cm^{-2} ($\hat{v}_{os} < v_{th}$) in Table II apply. (iii) Table II gives an indication how, e.g., by using granulated materials, foams, or by seeding, laser-matter coupling with ultrashort laser pulses can be improved and thermal electron transport is altered. In collisionless PIC simulations the effect is automatically included. An estimate of the lifetimes of clusters can be found in [17].

*Electronic address: Peter.Mulser@physik.tu-darmstadt.de
†Deceased.

[1] *Molecules and Clusters in Intense Laser Fields*, edited by J. Posthumus (Cambridge University Press, Cambridge, England, 2001), Chaps. 5–7.
[2] D. Bauer, J. Phys. B **37**, 3085 (2004); D. Bauer and A. Macchi, Phys. Rev. A **68**, 033201 (2003).
[3] U. Saalmann and J.-M. Rost, Phys. Rev. Lett. **91**, 223401 (2003).
[4] T. Ditmire, Phys. Rev. A **57**, R4094 (1998).
[5] F. Greschik, L. Dimou, and H.-J. Kull, Laser Part. Beams **18**, 367 (2000).
[6] Ch. Jungreuthmayer *et al.*, Phys. Rev. Lett. **92**, 133401 (2004).
[7] T. Taguchi, Th. M. Antonsen, Jr., and H. M. Milchberg, Phys. Rev. Lett. **92**, 205003 (2004).
[8] J. Bréchignac and J. P. Connerade, J. Phys. B **27**, 3795 (1994).
[9] T. Ditmire *et al.*, Phys. Rev. A **53**, 3379 (1996); Jiansheng Liu *et al.*, Phys. Rev. A **64**, 033426 (2001).
[10] S. V. Fomichev, D. F. Zaretsky, and W. Becker, J. Phys. B **37**, L175 (2004).
[11] P. B. Parks *et al.*, Phys. Rev. A **63**, 063203 (2001).
[12] F. Greschik, Ph.D thesis, Rheinisch Westfaelische Technische Hochschule, Aachen, 2002.
[13] T. Ditmire *et al.* in *Super-Strong Fields in Plasmas*, edited by M. Lontano *et al.*, AIP Conference Proceedings No. 426 (American Institute of Physics, New York, 1998), p. 354.
[14] M. H. R. Hutchinson *et al.* in *Super-Strong Fields in Plasmas*, edited by Lontano *et al.*, AIP Conference Proceedings No. 426 (American Institute of Physics, New York, 1998), p. 314.
[15] I. Yu. Kostyukov, JETP Lett. **73**, 393 (2001).
[16] P. Mulser *et al.*, Phys. Rev. E **63**, 016406 (2000).
[17] M. Kanapathipillai *et al.*, Phys. Plasmas **11**, 3911 (2004).
[18] Th. Bornath *et al.*, Phys. Rev. E **64**, 026414 (2001).
[19] R. Schneider, Contrib. Plasma Phys. **41**, 315 (2001).